

Synthesis and Photoinduced Intermolecular Electronic Acceptor Ability of Pyrazolo[60]fullerenes vs Tetrathiafulvalene

Juan Luis Delgado, Pilar de la Cruz, Vicente López-Arza, Fernando Langa,* Zhenhai Gan,[1] Yasuyuki Araki,[1] and Osamu Ito*,[1]

Facultad de Ciencias del Medio Ambiente, Universidad de Castilla-La Mancha, 45071, Toledo, Spain

[1]Institute of Multidisciplinary Research for Advanced Materials, Tohoku University, Katahira, Aoba-ku, Sendai 980-8577

Received January 12, 2005; E-mail: Fernando.LPuente@uclm.es, ito@tagen.tohoku.ac.jp

The synthesis of three novel pyrazolo[60]fullerene derivatives containing electron-withdrawing substituents has been described. High solubility in ordinary organic solvents was proved. Their electrochemical properties of pyrazolo-[60]fullerenes showed better electron affinity than pristine C_{60} in the ground state. The nanosecond transient absorption spectra showed clear evidence for photoinduced electron transfer from TTF to the excited triplet state of the pyrazolo-[60]fullerenes, in which stronger electron-withdrawing substituents accelerate the rates of the photoinduced electron-transfer, indicating a high electron-acceptor ability of the excited triplet state of pyrazolo[60]fullerenes.

One of the most outstanding applications of fullerenes is the preparation of photovoltaic cells as a result of their electron acceptor ability;[1,2] composite films of polymers derived from poly(phenylenevinylene) (PPV) and C_{60} present high efficiency,[3] which is caused by intermolecular photoinduced electron transfer (PET) from the donor to C_{60} (the acceptor) as a key process.[4] Nevertheless, the limited solubility of pristine C_{60} in organic solvents and its tendency to crystallize during film formation prevent its use in high-concentration blends.[5] To overcome these problems, a series of soluble C_{60} derivatives has been developed;[6] however, most of the C_{60} derivatives decrease the electron-acceptor properties compared with C_{60} as a result of the saturation of a double bond of the C_{60} cage, raising the LUMO energy.[7] Thus, attempts to increase the electron affinity of C_{60}, looking for a more efficient behavior in the charge-transfer and photoinduced electron-transfer processes, have been performed by many research groups, and better electron-affinities than pristine C_{60} have been found in several types of C_{60}-compounds.[8,9] On the other hand, we have shown that the 1,3-dipolar cycloaddition of nitrile imines, generated in situ from hydrazones,[10] is a general and versatile procedure to prepare pyrazolo[60]fullerenes (pyrazolo-C_{60}). In contrast with other families of fullerene derivatives, molecules based on pyrazolo-C_{60} derivatives present a similar electron affinity to pristine C_{60} as a consequence of the $-I$ effect of the nitrogen atom close to the C_{60} cage.[11]

In the present study, we focus on the preparation of a series of soluble pyrazolo-C_{60} derivatives (**2a–c**) bearing electron-withdrawing substituents, with the aim of improving the electron-acceptor ability of the C_{60} cage. The electrochemical and photophysical properties of the newly prepared pyrazolo-C_{60} derivatives **2a–c** have been studied in the both absence and presence of strong electron donors, such as the tetrathiafulvalene (TTF), in order to test their ability to be used as the acceptor partner in photovoltaic cells. The electrochemical properties of **2a–c** were measured by means of cyclic voltammetry (CV) and Osteryoung square-wave voltammetry (OSWV) techniques, which gave useful information about the acceptor ability of pyrazolo-C_{60} derivatives in the ground state, when compared with the parent C_{60}. In addition, we report a photophysical evidence that shows efficient intermolecular electron-transfer of the excited triplet states of these derivatives from TTF, by measuring the transient absorption spectra in the vis and near-IR regions after nanosecond laser light irradiation in a polar solvent.

Results and Discussion

Synthesis of Pyrazolo[60]fullerenes. Pyrazolo[60]fullerenes **2a–c** were synthesized in two steps from the corresponding aldehydes, as shown in Scheme 1. Hydrazones **1a–c** were prepared in 68–83% yield by a reaction of the corresponding aldehyde with 4-nitrophenylhydrazine in the presence of acetic acid using ethanol as a solvent. Cycloadducts **2a–c** were prepared by a modification of our previously described procedure.[12] The corresponding hydrazone was treated with *N*-bromosuccinimide (NBS) in chloroform at room temperature for 30 min; after removing the solvent in vacuo, the resulting bromo-derivative was reacted with Et_3N and C_{60} in toluene (see Experimental Section). The pyrazolo-C_{60} derivatives **2a–c** were obtained in 25–42% yield after purification by column chromatography (silica gel, toluene), followed by centrifugation in methanol and diethyl ether.

The structures of hydrazones **1a–c** and the C_{60}-cycloadducts **2a–c** were confirmed by analytical and spectroscopic data. The ^{1}H NMR spectra of **2a–c** in $CDCl_3$ exhibit all of the expected signals corresponding to the organic addend. A low field shift for the *ortho* protons ($\Delta\delta = 1.0$–1.1 ppm in the *N*-aryl group and 0.6–0.7 ppm in the *C*-aryl group) compared to the corresponding hydrazone was observed. Although it has been suggested that these low-field shifts are due to an intramolecular

Published on the web August 4, 2005; DOI 10.1246/bcsj.78.1500

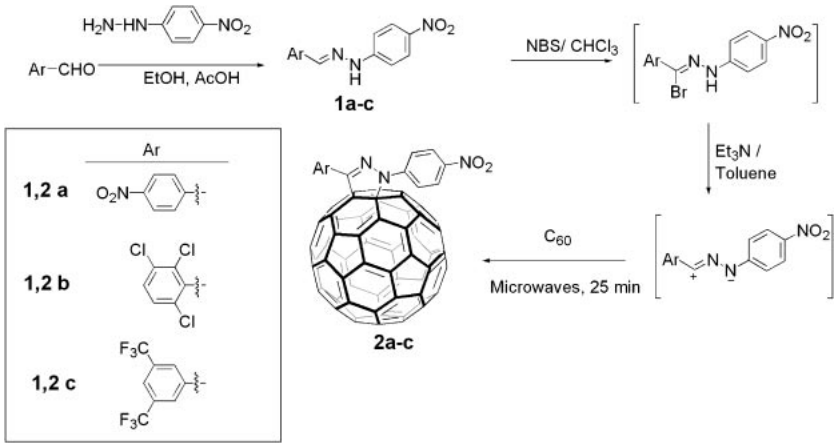

Scheme 1.

Table 1. Solubility, in mol dm^{-3}, of **2a–c** and C_{60} in Several Solvents at Room Temperature

Solvents	Compounds			
	C_{60}[a)]	**2a**	**2b**	**2c**
Dichloromethane	3.6×10^{-4} a)	1.0×10^{-3}	1.6×10^{-3}	2.6×10^{-3}
Acetone	1.4×10^{-6}	—b)	5.8×10^{-5}	1.2×10^{-4}
Diethyl Ether	—b)	—b)	4.5×10^{-5}	4.7×10^{-4}
Methanol	—b)	—b)	—b)	2.9×10^{-5}

a) According to Ref. 15b. b) Less than 1.0×10^{-6} mol dm^{-3}.

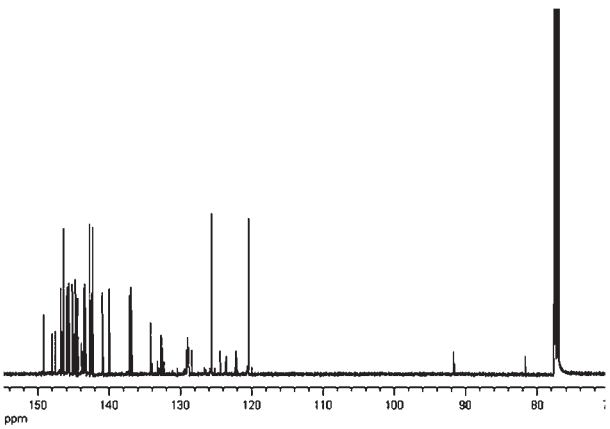

Fig. 1. ^{13}C NMR spectrum of **2b** in $CDCl_3$.

charge-transfer (CT) interaction between the benzene ring and the C_{60} cage,[13] it seems that the strong anisotropic effect of the fullerene is the origin of this low field-shift.[14] The electron-withdrawing nature of the substituents in **2a–c** supports this hypothesis. The observed signals in the ^{13}C NMR spectra are in agreement with the proposed structures showing the signals originated from the substituted pyrazoline moiety as well as most from the C_{60} system with the appearance of the sp^3 carbons of the C_{60} cage in the range of 81–91 ppm (Fig. 1). The structures of **2a–c** were also confirmed by MALDI-TOF mass spectra, which show the expected MH^+ peaks at $m/z = 1063$ (**2a**), 1005 (**2b**), and 1096 (**2c**), together with several fragmentation peaks. The absorption spectra of **2a–c** are similar to those described for other pyrazolo-C_{60} derivatives showing the band at 427 nm, which is typical of [6,6]adducts.[11]

Solubility. It is well documented that the solubility of C_{60} is quite low in most common solvents.[15] In fact, C_{60} is totally insoluble in polar solvents, like as acetone or methanol.[15] This low solubility limits its use in various devices, such as photovoltaic cells, due to its strong tendency to crystallize in the procedures to prepare films. To overcome this problem, soluble fullerene derivatives are needed. Interesting studies have been made by several groups in order to obtain highly soluble fullerene derivatives in water or other solvents.[16] In the present study, we determined the solubility of the pyrazolo-C_{60} derivatives **2a–c** in polar and nonpolar solvents by UV–vis spectroscopy. Standard solutions of **2a–c** in the studied solvents were prepared to obtain a linear calibration line of absorbance vs concentration under dilute concentration. Saturated solutions of all compounds were then prepared and centrifugated to obtain clear solutions. After dilution, the solubility was determined by interpolation using the calibration line; the results are collected in Table 1. In dichloromethane, in which pristine C_{60} shows the best solubility among the ordinal organic solvents, better solubility of **2a–c** by factors of 3–7 was observed. In polar acetone, which shows low solubility for pristine C_{60}, **2b** and **2c** showed higher solubility by factors of 40–80. In diethyl ether and methanol, in which pristine C_{60} is scarcely soluble ($<10^{-6}$ mol dm^{-3}), a solubility of more than 2.9×10^{-5}–4.7×10^{-4} mol dm^{-3} was observed for **2c**. For **2c**, the solubility increases in the order of methanol < acetone < diethyl ether < dichloromethane. The high solubility of the pyrazolo-C_{60} derivatives in these solvents should be very valuable in preparing homogeneous films in devices.

Electrochemistry. The electrochemical behavior of the newly synthesized pyrazolo-C_{60} derivatives was examined using cyclic voltammetry (CV) and Osteryoung square-wave

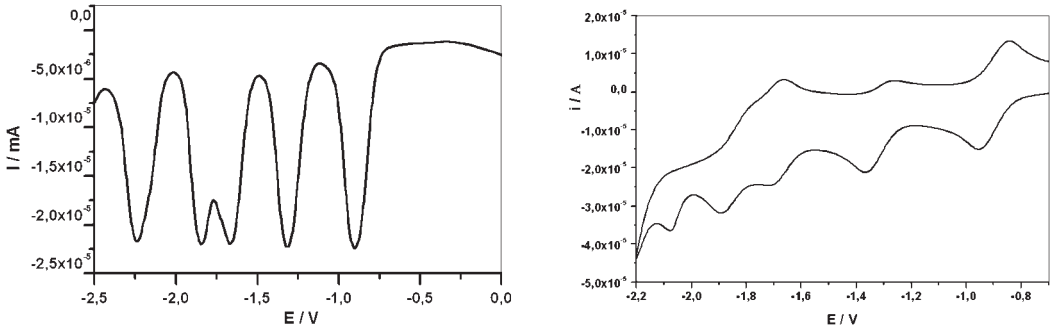

Fig. 2. OSWV (left) and cyclic voltammogram (right) of compound **2c** in *o*-dichlorobenzene/acetonitrile (4:1) (V vs $Ag/AgNO_3$; scan rate was 100 mV s^{-1}).

Table 2. Reduction Potentials (V)[a)] Determined by OSWV of **2a–c** and C_{60} Measured in *o*-Dichlorobenzene/Acetonitrile (4:1)

Compound	E^1_{red}	E^2_{red}	E^3_{red} b)	E^4_{red} b)	E^5_{red}	E^6_{red}
C_{60}	−0.960	−1.368			−1.837	−2.303
2a	−0.910	−1.318	−1.512	−1.722	−1.932	−2.381
2b	−0.927	−1.331		−1.780	−1.862	−2.175
2c	−0.892	−1.310		−1.660	−1.839	−2.230

a) V vs $Ag/AgNO_3$; GCE as working electrode; 0.1 mol dm^{-3} TBAP; scan rate was 100 mV s^{-1}.
b) Irreversible according to cyclic voltammetry, corresponds to the nitrobenzene group.

voltammetry (OSWV) techniques at room temperature, as shown in Fig. 2 for **2c**. These studies were carried out in *o*-dichlorobenzene/acetonitrile (4:1) as a solvent and using tetrabutylammonium perchlorate (TBAP) as a supporting electrolyte (see Experimental Section). Data obtained by the OSWV technique are collected in Table 2 along with those of pristine C_{60} for the sake of a comparison; **2b** and **2c** show four quasi-reversible reduction potentials, which are assigned to the C_{60} cage.[17] For **2a**, additional non-reversible reduction potentials are situated between the second and third potentials of the C_{60} cage (Fig. 2); this additional reduction wave is assigned to the reduction of the nitrophenyl group. Pyrazolo-C_{60} derivatives **2a–c** show values of the first reduction potential with slightly less negative values (33–66 mV) than that of C_{60}, indicating a higher electron affinity than pristine C_{60} in the ground states. The E^1_{red} values shift to less negative in the order of **2c** (CF_3) < **2a** (NO_2) < **2b** (Cl).

Steady-State Absorption and Fluorescence Spectra. The UV–vis spectra of **2a** and the mixture of **2a** with TTF in *o*-dichlorobenzene are shown in Fig. 3; the weak peak at 685 nm and broad absorption band in the 600–500 nm region with intermediate intensity are characteristic of C_{60} derivatives. The absorption bands in 350–500 nm are an overlapping of the C_{60} and nitrobenzene moieties. Almost the same absorption spectra were observed for **2b** and **2c**. The solvent-polarity effect on these absorption spectra was small. Upon the addition of TTF, the absorption bands at 460 nm and 355 nm are attributed to TTF (Fig. 3). In the 510–720 nm region, no appreciable change was observed upon the addition of TTF. This suggests that the interaction between **2a** (0.05 mmol dm^{-3}) and excess TTF (0.5 mmol dm^{-3}) is quite weak. Similar absorption spectra were observed for a mixture of **2b**/**2c** and TTF in *o*-dichlorobenzene and in benzonitrile. The absorption maxima in the longest wavelength region are listed in Table 3. In the fluorescence spectra and transient absorption experiments, as described in a later part of this report, a 532-nm laser-light was employed to selectively excite the C_{60} moiety of **2a–c** without the excitation of TTF.

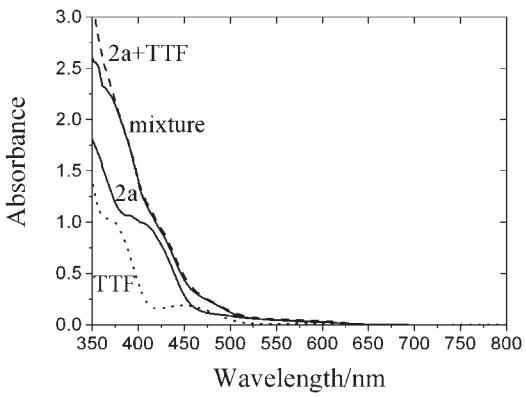

Fig. 3. Steady-state absorption spectra of **2a** (0.05 mmol dm^{-3}), TTF (0.5 mmol dm^{-3}), and mixture of **2a** (0.05 mmol dm^{-3}) and TTF (0.5 mmol dm^{-3}), and added spectra (**2a** + TTF) in *o*-dichlorobenzene.

The fluorescence spectra of **2a** and a mixture of **2a** with TTF in *o*-dichlorobenzene observed by 532 nm light excitation are shown in Fig. 4. For **2a**, a fluorescence peak was observed at 695 nm with a shoulder at 770 nm; the fluorescence peaks are almost a mirror image of the absorption in the 650–700 nm region. Thus, the fluorescence peak at 695 nm with a shoulder at 770 nm arises from the C_{60} moiety of **2a**. Almost the same fluorescence spectra were observed for **2b** and **2c** in *o*-dichlorobenzene and in other organic solvents. The fluorescence peaks are summarized in Table 3. Upon the addition of excess TTF, no appreciable change was observed (Fig. 4).

Table 3. Spectroscopic Data for **2a–c** and C_{60}; Longest Absorption Maxima ($\lambda_{abs,max}$), Fluorescence Peak ($\lambda_{F,max}$), and Lifetime (τ_F) in *o*-Dichlorobenzene; Triplet–Triplet Absorption Maxima ($\lambda_{abs,max}{}^{T}$) in Toluene and Absorption Maxima of Radical Anion ($\lambda_{abs,max}{}^{A}$) in Benzonitrile

Compound	$\lambda_{abs,max}$/nm	$\lambda_{F,max}$/nm	τ_F/ns	$\lambda_{abs,max}{}^{T}$/nm	$\lambda_{abs,max}{}^{A}$/nm
C_{60}	624	697	1.30	740	1080
2a	691	695	1.46	700	1060
2b	691	697	1.43	700	1080
2c	686	686	1.48	700	1040

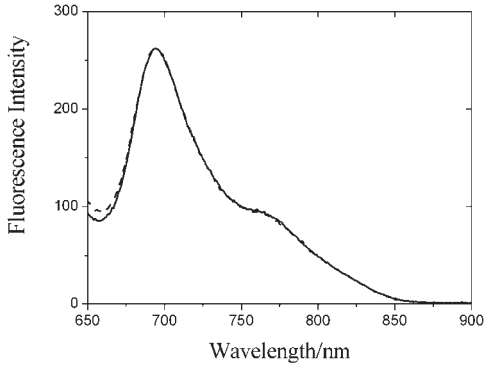

Fig. 4. Steady-state fluorescence spectra of **2a** (0.05 mmol dm^{-3}; solid line) and mixture (dotted line) of **2a** (0.05 mmol dm^{-3}) and TTF (0.5 mmol dm^{-3}) observed with excitation wavelength at 532 nm in *o*-dichlorobenzene.

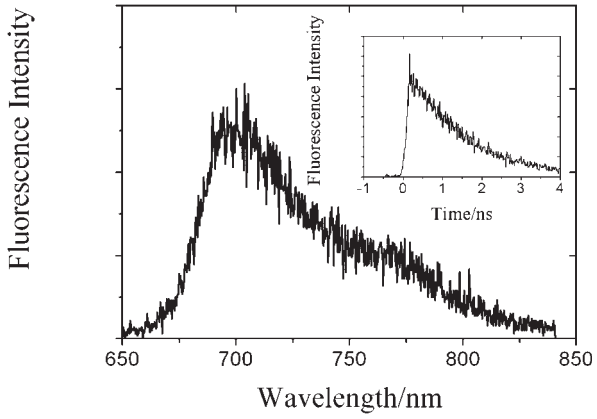

Fig. 5. Time-resolved fluorescence spectra of **2a** (0.05 mmol dm^{-3}) observed with excitation wavelength at 400 nm in THF. Inset: Time profile at 700 nm.

This suggests that in such a dilute solution (**2a–c**, 0.05 mmol dm^{-3} and TTF, 0.5 mmol dm^{-3}), the interaction between the excited singlet state of **2a** and excess TTF is quite weak in *o*-dichlorobenzene. A similar behavior was observed for a mixture of **2b–c** and TTF in *o*-dichlorobenzene and in benzonitrile.

Time-Resolve Fluorescence Measurements. Time-resolved fluorescence spectra and time profiles of **2a–2c** were observed. In Fig. 5, the fluorescence spectra and time profiles of **2a** are shown. The fluorescence spectrum is almost the same at longer wavelengths than the peak region (680–850 nm), while in a shorter wavelength region than 675 nm, a slight difference was observed, probably due to stray light in the steady-state fluorescence measurements. From the time profiles, which obey a single exponential function, the fluorescence lifetimes (τ_F) of **2a–2c** were evaluated, as listed in Table 3. The τ_F values of **2a–2c** are almost the same as that of pristine C_{60} and the reported τ_F values for other C_{60} derivatives.[18]

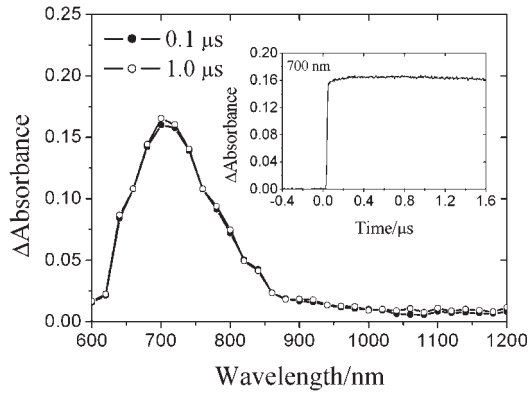

Fig. 6. Nanosecond transient absorption spectra observed by the excitation of **2c** (0.5 mmol dm^{-3}) with 532 nm laser-light in Ar-saturated benzonitrile.

Nanosecond Transient Absorption Spectra. Figure 6 shows the transient absorption spectra observed by the excitation of **2c** with the 532 nm laser light in toluene. The peak at 700 nm is characteristic of the triplet–triplet transition of the C_{60} moiety.[19] In an Ar-saturated toluene solution, the decay at 700 nm was slow living until ca. 50 μs; from longer time-scale measurements, the lifetime of the triplet state of the C_{60} moiety of **2c** (^{3}**2c***) was evaluated to be ca. 30 μs. Upon the addition of O_2, the 700 nm band decayed quickly, indicating that the triplet energy of **2c** transfers to O_2. Similar transient spectra and time profiles were observed for **2a** and **2b**. These observations confirmed the formation of ^{3}**2***, which may be produced via intersystem crossing (ISC) from the excited singlet states of **2a–c** (^{1}**2***) having a shorter lifetime than a nanosecond laser pulse (6 ns in our instrument). In **2a–c**, without an electron-donating group, intramolecular charge separation does not take place, although for pyrazolo-C_{60} derivatives with the electron-donating groups, the intramolecular charge separation was observed.[20] The absorption maxima of ^{3}**2*** are listed in Table 3.

Figure 7 shows the transient absorption spectra observed by the excitation of **2c** with 532-nm laser-light in the presence of TTF in Ar-saturated benzonitrile. Immediately after laser-light excitation, the transient absorption band of ^{3}**2c*** was mainly observed. With a concomitant decay of the 700 nm band, a new absorption band appeared at 1040 nm, which can be attributed to the radical anion of the C_{60} moiety (**2c**$^{\bullet-}$); the ab-

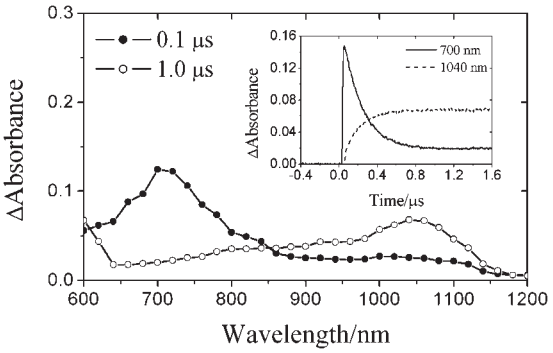

Fig. 7. Nanosecond transient absorption spectra observed by the excitation of **2c** (0.5 mmol dm^{-3}) with 532 nm laser-light in the presence of TTF (0.5 mmol dm^{-3}) in Ar-saturated benzonitrile; (●) 100 ns and (○) 1000 ns. Inset: Time profiles at 700 and 1040 nm.

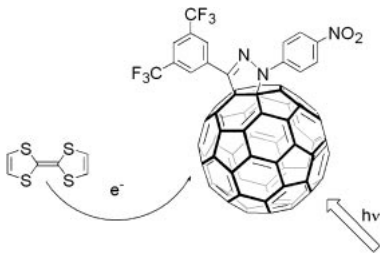

Scheme 2.

sorption peaks of **2c**$^{\bullet-}$ are listed in Table 3. These observations clearly indicated that electron transfer takes place via ^{3}**2c*** as Eq. 1 and Scheme 2.[19] In the transient spectrum observed at 1.0 μs, an absorption tail was observed in the 600–640 nm region, which may be attributed to the radical cation of TTF (TTF$^{\bullet}$).[21]

$$^3\mathbf{2}^* + \mathrm{TTF} \xrightarrow{k_{ET}} \mathbf{2}^{\bullet-} + \mathrm{TTF}^{\bullet+}. \quad (1)$$

In the time profiles inserted in Fig. 7, the decay of ^{3}**2c*** increased on the addition of TTF; with this rapid decay, a rise of **2c**$^{\bullet-}$ was observed. These decays and rise rates increased with the concentration of TTF, as shown in Fig. 8.

These decays and rises were curve-fitted with a single exponential, from which the first-order rate constants ($k_{\text{first-order}}$) were evaluated. The $k_{\text{first-order}}$ values increased linearly with the TTF concentration, as shown in Fig. 9 for the **2c**–TTF solution. The plots for the decay rates of ^{3}**2c*** are almost the same as those for the rise rates of **2c**$^{\bullet-}$ within the experimental errors, giving the same slope, from which the second-order rate constants (k_q) were evaluated as 2.2×10^9 mol^{-1} dm^3 s^{-1}. For **2a**–TTF and **2b**–TTF solutions, the k_q values were evaluated as listed in Table 4. The k_q values increase slightly in the order of **2a** (NO_2) < **2b** (Cl) < **2c** (CF_3).

The efficiency of electron transfer via ^{3}**2*** can be evaluated by the ratio of the maximal absorbance of **2**$^{\bullet-}$ ($A_{\mathbf{2}^{\bullet-},\max}$) to the initial absorbance of ^{3}**2*** ($A_{^3\mathbf{2}^*,\text{initial}}$). This ratio increases with the TTF concentration, saturating at TTF = ca. 1.0 mmol dm^{-3}, as shown in Fig. 10. Upon assuming the molar extinction coefficients for the absorption band of **2**$^{\bullet-}$ at ca. 1000 nm (ε_A) and the absorption band of ^{3}**2*** at ca. 700 nm (ε_T) to

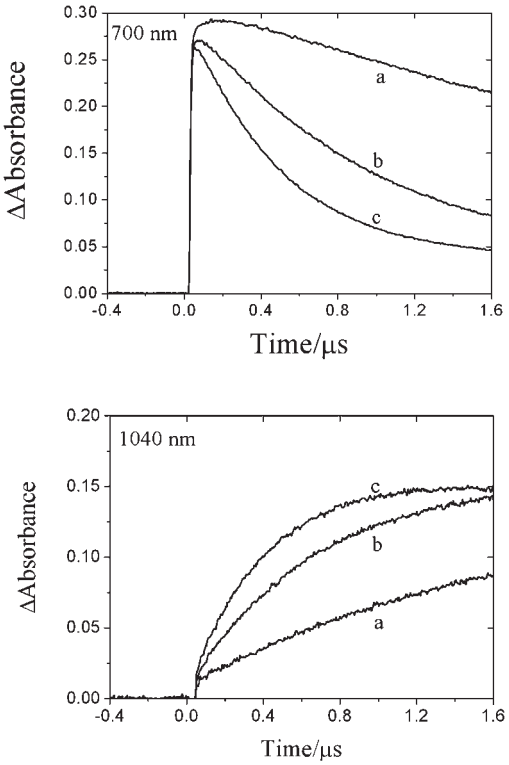

Fig. 8. Time profiles at (A) 700 nm and (B) 1040 nm for **2c** with changing TTF concentrations; [TTF] = (a) 0.2, (b) 0.5, and (c) 1.0 mmol dm^{-3}. Other conditions were the same as Fig. 6.

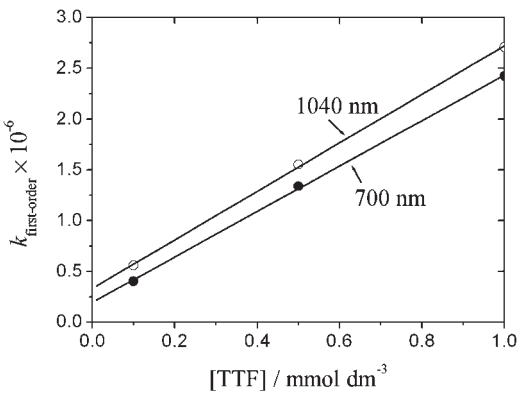

Fig. 9. Plots of $k_{\text{first-order}}$ vs [TTF] for the decay of ^{3}**2c*** at 700 nm and rise of **2c**$^{\bullet-}$ at 1040 nm.

Table 4. Quenching Rate Constants (k_q) of ^{3}**2*** by TTF, Quantum Yield (Φ_{ET}) and Rate Constant (k_{ET}) for Forward Electron Transfer via ^{3}**2*** from TTF, and Back Electron-Transfer Rate-Constants (k_{BET}) between **2**$^{\bullet-}$ and TTF$^{\bullet+}$ in Benzonitrile

Acceptor	k_q/ mol^{-1} dm^3 s^{-1}	Φ_{ET}	k_{ET}/ mol^{-1} dm^3 s^{-1}	k_{BET}/ mol^{-1} dm^3 s^{-1}
2a	1.8×10^9	0.54	1.0×10^9	8.6×10^9
2b	2.0×10^9	0.66	1.3×10^9	8.3×10^9
2c	2.2×10^9	0.70	1.5×10^9	8.2×10^9

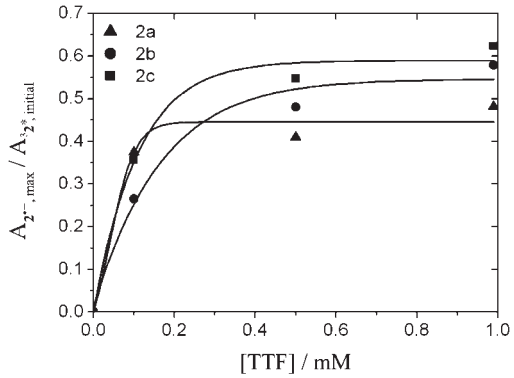

Fig. 10. Plots of $A_{2^{\bullet-},max}/A_{^32^*,initial}$ vs [TTF]; for $^32^*$ at 700 nm and for $2^{\bullet-}$ at 1040–1080 nm.

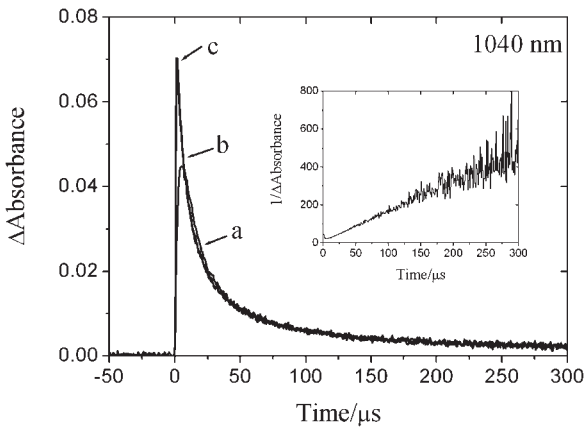

Fig. 11. Longer time-scale of decay curves at 1040 nm of $2c^{\bullet-}$ generated by laser-light excitation of **2c** (0.1 mmol dm^{-3}) in the presence of TTF: [TTF] = (a) 0.1, (b) 0.5, and (c) 1.0 mmol dm^{-3} in Ar-saturated benzonitrile. Inset: Plot of second-order kinetics.

be 5000 and 6000 cm^{-1} mol^{-1} dm^3, respectively,[18] the quantum yields (Φ_{ET}) of electron transfer via $^32^*$ (Φ_{ET}) were evaluated to be 0.54–0.70. The Φ_{ET} values increase in the order of **2a** (NO_2) < **2b** (Cl) < **2c** (CF_3). Thus, the k_{ET} values were finally obtained from the relation $k_{ET} = \Phi_{ET} \cdot k_q$, as listed in Table 4. The k_{ET} values increase in the order of **2a** (NO_2) < **2b** (Cl) < **2c** (CF_3).

In long time-scale measurements, $2^{\bullet-}$ began to decay, obeying second-order kinetics (inset in Fig. 11), which indicates that the back electron transfer takes place between $2^{\bullet-}$ and $TTF^{\bullet+}$ after both radical ions are solvated by benzonitrile. The time profiles are almost the same with increasing TTF concentration, as shown in Fig. 11. The slope of the second-order plot gave the ratio of the back electron transfer rate constant (k_{BET}) to the ε_A values. Upon employing $\varepsilon_A = 5000$ cm^{-1} mol^{-1} dm^3, the k_{BET} values close to the diffusion-controlled limit in benzonitrile were evaluated (Table 4). This finding indicates that the photoinduced processes complete without side reactions.

Conclusion

A series of newly synthesized pyrazolo[60]fullerenes bearing electron-withdrawing substituents showed an improved solubility and electron affinity compared with pristine C_{60}. By laser flash photolysis, the electron-transfer process from TTF to the excited triplet states of pyrazolo[60]fullerenes was confirmed; the rate constants for electron transfer increase in the order of **2a** (NO_2) < **2b** (Cl) < **2c** (CF_3).

Experimental

General Remarks. All cycloaddition reactions were performed under argon. C_{60} was purchased from MER Corporation (Tucson, AZ); TLC using Merck silica gel 60-F254 was employed to monitor cycloaddition reactions. ^{1}H NMR and ^{13}C NMR spectra were recorded on a Varian Mercury 200 apparatus. UV–vis absorption spectra were obtained on a Shimadzu spectrophotometer. FT-IR spectra were recorded on a Nicolet Impact 410 spectrophotometer using KBr disks. MALDI-TOF mass spectra were obtained on a Bruker ReflexIII spectrometer. Cyclic voltammetry measurements were carried out on an Autolab PGSTAT 30 potentiostat using a BAS MF-2062 Ag/0.01 mol dm^{-3} $AgNO_3$ as a reference electrode, an auxiliary electrode consisting of a Pt wire, and a Metrohm 6.1247.000 conventional glassy carbon electrode (GCE, 3 mm o.d.) as a working electrode, directly immersed in the *o*-dichlorobenzene/acetonitrile solution containing 0.1 mol dm^{-3} TBAP as an electrolyte. A 10 mL electrochemical cell from BAS, Model VC-2, was also used. The reference potential was shifted by 290 mV towards a more negative potential compared with the Ag/AgCl scale. $E_{1/2}$ values were taken as the average of the anodic and cathodic peak potentials. The scan rate was 100 mV s^{-1}.

Steady-state absorption spectra were measured on a JASCO V-530 UV–vis spectrophotometer. Steady-state fluorescence spectra were measured on a Shimadzu RF-5300 PC spectrofluorophotometer. Fluorescence lifetimes were measured by a single-photon counting method using a second harmonic generation (SHG, 410 nm) of a Tisapphire laser [Spectra–Physics, Tsunami 3950-L2S, 1.5 ps full width at half-maximum (fwhm)] and a streak scope (Hamamatsu Photonics, C4334-01) equipped with a polychromator (Action Research, SpectraPro 150) as an excitation source and a detector, respectively. Nanosecond transient absorption spectra were measured using pulsed laser light from an optical parametric oscillation (Continuum Surelite OPO, fwhm 6 ns) pumped by a Nd:YAG laser (Continuun, Surelite II-10). For measurements of the transient absorption spectra in the near-IR region, a Ge avalanche photodiode (APD, Hamamatsu Photonics, B2834) was used as a detector for monitoring light from a pulsed xenon lamp.[22]

General Synthesis Procedure of Hydrazones. A solution of the corresponding aldehyde (6.52 mmol), 4-nitrophenylhydrazine (6.52 mmol) and two drops of acetic acid in 10 mL of ethanol was heated under reflux for 10 min. After the mixture was cooled to room temperature, the solid was filtered. Then, the solid was recrystallized from ethanol.

4-Nitrobenzaldehyde 4-Nitrophenylhydrazone (1a). Yield: 83%. mp 245–247 °C. FT-IR (KBr) ν/cm^{-1} 526, 685, 745, 844, 1268, 1494, 1560, 1687, 2362. ^{1}H NMR ($CDCl_3$) δ/ppm 7.2 (d, 2H, J = 8.8 Hz), 7.84 (d, 2H, J = 8.4 Hz), 8.23 (d, 2H, J = 8.4 Hz), 8.26 (s, 1H), 8.28 (d, 2H, J = 8.8 Hz). ^{13}C NMR (DMSO) δ/ppm 111.3, 123.3, 125.4, 126.4, 138.2, 138.5, 140.4, 146.2, 149.1. MALDI MS: m/z: 285.8. Anal. calcd for $C_{13}H_{10}N_4O_4$: C, 54.55; H, 3.52; N, 19.57%. Found: C, 54.15; H, 3.31; N, 19.72%.

2,3,6-Trichlorobenzaldehyde 4-Nitrophenylhydrazone (1b). Yield 68%. mp 225–227 °C. FT-IR (KBr) ν/cm^{-1} 592, 751, 851, 871, 957, 1461, 1560, 1786, 1859, 1918. ^{1}H NMR ($CDCl_3$)

δ/ppm 7.2 (d, 2H, $J = 9.2$ Hz), 7.3 (d, 1H, $J = 8.8$ Hz), 7.4 (d, 1H, $J = 8.8$ Hz), 8.1 (s, 1H), 8.2 (d, 2H, $J = 9.2$ Hz), 8.3 (s, 1H), 8.4 (s, 1H). ^{13}C NMR (DMSO) δ/ppm 111.7, 123.8, 125.8, 126.8, 126.9, 138.6, 138.9, 146.6, 149.6. Anal. calcd for $C_{13}H_8Cl_3N_3O_2$: C, 45.31; H, 2.34; N, 12.19%. Found: C, 45.47; H, 2.16; N, 12.03%.

3,5-Bis(trifluoromethyl)benzaldehyde 4-Nitrophenylhydrazone (1c). Yield: 71%. mp 259–261 °C. FT-IR (KBr) ν/cm^{-1} 526, 692, 745, 831, 990, 1110, 1196, 1474, 1534, 1587, 1706. ^{1}H NMR ($CDCl_3$) δ/ppm 7.2 (d, 2H, $J = 9.2$ Hz), 7.8 (s, 1H), 8.1 (s, 2H), 8.2 (d, 2H, $J = 9.2$ Hz), 8.45 (s, 1H). ^{13}C NMR ($CDCl_3$) δ/ppm 111.7, 125.7, 125.8, 126.1, 130.1, 130.8, 137.4, 137.8, 138.8, 149.8. Anal. calcd for $C_{15}H_9F_6N_3O_2$: C, 47.76; H, 2.40; N, 11.14; O, 8.48%. Found: C, 47.69; H, 2.42; N, 11.08%.

General Synthesis Procedure of Cycloadducts. A solution of NBS (0.26 mmol) and the corresponding hydrazone (0.17 mmol) in $CHCl_3$ was stirred at room temperature for 30 min. The solvent was removed in vacuo, and a solution of C_{60} (0.13 mmol) and Et_3N (0.21 mmol) in toluene (50 mL) was added to the solid. The mixture was treated according to the described process for each compound. After the corresponding reaction time, the solvent was removed under reduced pressure. The resulting solid was purified by silica-gel flash chromatography using toluene as eluent. Centrifuging three times with methanol and once with diethyl ether accomplished further purification of the solid.

1′,3′-Bis(4-nitrophenyl)pyrazolo[4′,5′-*a*][60]fullerene (2a). The solution was irradiated by microwave for 30 min at 210 W of power. Yield 25% (72% based on recovered C_{60}). FT-IR (KBr) ν/cm^{-1} 527, 718, 1182, 1421, 1494, 1547, 1653, 1699. ^{1}H NMR ($CDCl_3$) δ/ppm 8.3 (d, 2H, $J = 9.5$ Hz), 8.38 (d, 2H, $J = 9.5$ Hz), 8.41 (d, 2H, $J = 8.7$ Hz), 8.5 (d, 2H, $J = 8.7$ Hz). ^{13}C NMR ($CDCl_3$) δ/ppm 81.5, 91.0, 109.4, 119.7, 123.8, 125.0, 129.7, 136.2, 136.7, 137.5, 139.4, 140.4, 141.7, 141.8, 142.0, 142.2, 142.3, 142.8, 143.0, 143.94, 144.1, 144.2, 144.8, 145.0, 145.1, 145.3, 145.4, 145.8, 145.9, 146.0, 146.2, 146.3, 147.0, 147.4, 147.9, 148.5. UV–vis (benzonitrile) λ_{max}/nm ($\log \varepsilon$) 323 (4.58), 415 (4.26), 682 (2.17). MS m/z: 1005.0 (M + 1), 720.1 (C_{60}).

1′-(4-Nitrophenyl)-3′-(2,3,6-trichlorophenyl)pyrazolo[4′,5′-*a*]-[60]fullerene (2b). The solution was stirred at room temperature for 30 min. Yield: 34% (78% based on recovered C_{60}). FT-IR (KBr) ν/cm^{-1} 513, 745, 851, 1109, 1481, 1600, 3417. ^{1}H NMR ($CDCl_3$) δ/ppm 7.5 (d, 1H, $J = 8.8$ Hz), 7.6 (d, 1H, $J = 8.8$ Hz), 8.2 (d, 2H, $J = 9.5$ Hz), 8.3 (d, 2H, $J = 9.5$ Hz). ^{13}C NMR ($CDCl_3$) δ 81.4, 91.3, 120.2, 121.9, 123.3, 124.0, 125.3, 125.4, 128.2, 128.6, 128.7, 129.0, 132.0, 132.3, 132.5, 132.8, 136.6, 139.6, 139.9, 140.6, 141.9, 142.0, 142.2, 142.4, 143.0, 143.1, 143.2, 143.3, 143.5, 144.2, 144.3, 144.4, 144.8, 144.9, 145.3, 145.4, 145.5, 145.6, 146.0, 146.1, 146.2, 146.4, 146.5, 147.2, 147.7, 149.0. UV–vis (benzonitrile) λ_{max}/nm ($\log \varepsilon$) 326 (4.61), 370 (4.43), 487 (3.26), 687 (2.34). MS m/z: 1063.0 (M + 1), 720.1 (C_{60}).

3′-[3,5-Bis(trifluoromethyl)phenyl]-1′-(4-nitrophenyl)pyrazolo[4′,5′-*a*][60]fullerene (2c). The solution was irradiated by microwave for 25 min at 210 W of power. Yield: 42% (92% based on recovered C_{60}). FT-IR (KBr) ν/cm^{-1} 526, 712, 824, 1169, 1315, 1454, 1494, 1587. ^{1}H NMR ($CDCl_3$) δ/ppm 8.0 (s, 1H), 8.3 (d, 2H, $J = 8.8$ Hz), 8.4 (d, 2H, $J = 8.8$ Hz), 8.8 (s, 2H). ^{13}C NMR ($CDCl_3$) δ/ppm 81.2, 91.2, 118.7, 120.1, 121.5, 123.1, 123.1, 124.2, 125.2, 126.9, 128.4, 132.1, 133.7, 136.5, 136.8, 139.5, 141.9, 142.3, 142.9, 142.9, 144.2, 144.2, 144.6, 145.2, 145.2, 145.4, 145.5, 145.9, 146.0, 146.4. UV–vis (benzonitrile) λ_{max}/nm ($\log \varepsilon$) 322 (4.56), 392 (4.28), 490 (3.19), 682 (2.16). MS m/z: 1095.9 (M + 1), 720 (C_{60}).

Financial support for this work was provided by grants from Ministerio de Educación y Ciencia of Spain and Feder funds (Project CTQ2004-00364/BQU) and Junta de Comunidades de Castilla-La Mancha (Project PAI-02-023). The authors (Y. A. and O. I.) are also grateful to financial supports by Grant-in-Aid for Scientific Researches on Priority Area (417) from Ministry of Education, Culture, Sports, Science and Technology of Japan.

References

1 a) N. S. Sariciftci, "Optical and Electronic Properties of Fullerenes and Fullerene-Based Materials," ed by J. Shinar, Z. V. Vardeny, and Z. H. Kafafi, Marcel Dekker Inc. (2000), Chap. 11. b) M. T. Rispens and J. C. Hummelen, "Fullerenes: From Synthesis to Optoelectronic Properties," ed by D. M. Guldi and N. Martin, Kluwer Academic Publishers (2002), Chap. 12.

2 N. Martín, L. Sánchez, B. Illescas, and I. Pérez, *Chem. Rev.*, **98**, 2527 (1998).

3 a) N. S. Saricifti, L. Smilowitz, A. J. Heeger, and F. Wudl, *Science*, **258**, 1474 (1992). b) B. Kraabel, J. C. Hummelen, D. Vacar, D. Moses, N. S. Saricifti, A. J. Heeger, and F. Wudl, *J. Chem. Phys.*, **104**, 4267 (1996). c) L. S. Roman, M. R. Anderson, T. Yohannes, and O. Inganas, *Adv. Mater.*, **9**, 1164 (1997).

4 a) H. Imahori and Y. Sakata, *Eur. J. Org. Chem.*, **64**, 2445 (1999). b) D. M. Guldi, *Chem. Commun.*, **2000**, 32. c) D. Gust, T. H. Moore, and A. L. Moore, *Acc. Chem. Res.*, **34**, 40 (2001). d) D. M. Guldi, *Chem. Soc. Rev.*, **31**, 22 (2002).

5 G. Yu, J. Gao, J. C. Hummelen, F. Wudl, and A. J. Heeger, *Science*, **270**, 1789 (1995).

6 J. C. Hummelen, B. W. Knight, F. LePeq, and F. Wudl, *J. Org. Chem.*, **60**, 532 (1995).

7 L. Echegoyen and L. E. Echegoyen, *Acc. Chem. Res.*, **31**, 593 (1998).

8 a) T. Da Ros, M. Prato, M. Carano, P. Ceroni, F. Paoulucci, and S. Roffia, *J. Am. Chem. Soc.*, **120**, 11645 (1998). b) D. M. Guldi and M. Prato, *Acc. Chem. Res.*, **33**, 695 (2000). c) D. M. Guldi, S. González, N. Martín, A. Antón, J. Garín, and J. Orduna, *J. Org. Chem.*, **65**, 1978 (2000). d) F. Hauke, A. Swartz, D. M. Guldi, and A. Hirsch, *J. Mater. Chem.*, **12**, 2088 (2002).

9 a) F. Langa, P. de la Cruz, E. Espíldora, A. González-Cortés, A. de la Hoz, and V. López-Arza, *J. Org. Chem.*, **65**, 8675 (2000). b) H. Irgartingen, P. W. Fettel, T. Escher, P. Tinnefeld, S. Nord, and M. Sauer, *Eur. J. Org. Chem.*, **3**, 455 (2000). c) B. Illescas and N. Martín, *J. Org. Chem.*, **65**, 5986 (2000). d) F. Li, Y. Li, B. Zhang, A. Shi, and D. Zhu, *Synth. Met.*, **102**, 1494 (1999).

10 a) P. de la Cruz, A. Díaz-Ortiz, J. J. García, M. J. Gómez-Escalonilla, A. de la Hoz, and F. Langa, *Tetrahedron Lett.*, **40**, 1587 (1999). b) F. Langa, P. de la Cruz, E. Espíldora, A. de la Hoz, J. L. Bourdelande, L. Sánchez, and N. Martín, *J. Org. Chem.*, **66**, 5033 (2001).

11 a) F. Langa, M. J. Gómez-Escalonilla, E. Diez-Barra, J. C. García-Martínez, A. de la Hoz, J. Rodríguez-López, A. González-Cortés, and V. López-Arza, *Tetrahedron Lett.*, **42**, 3435 (2001). b) F. Langa, P. de la Cruz, J. L. Delgado, M. J. Gómez-Escalonilla, A. González-Cortés, A. de la Hoz, and V. López-Arza, *New. J. Chem.*, **26**, 76 (2002).

12 E. Espíldora, J. L. Delgado, P. de la Cruz, A. de la Hoz,

V. López-Arza, and F. Langa, *Tetrahedron*, **58**, 5821 (2002).

13 Y. Matsubara, H. Tada, S. Nagase, and Z.-J. Yoshida, *J. Org. Chem.*, **60**, 5372 (1995).

14 F. Langa, P. de la Cruz, J. L. Delgado, E. Espíldora, M. J. Gómez-Escalonilla, and A. de la Hoz, *J. Mater. Chem.*, **12**, 2130 (2002).

15 a) R. S. Ruoff, D. S. Tse, R. Malhorta, and D. C. Lorents, *J. Phys. Chem.*, **97**, 3379 (1993). b) A. Hirsch, "The Chemistry of Fullerenes," Thieme Publishers (1994).

16 a) I. Texier, M. N. Berberan-Santos, A. Fedorov, A. Brettreich, H. Schonberger, A. Hirsch, S. Leach, and R. V. Bensasson, *J. Phys. Chem. A*, **105**, 10278 (2001). b) S. Bosi, L. Feruglio, D. Milic, and M. Prato, *Eur. J. Org. Chem.*, **24**, 4741 (2003). c) D. Felder, M. Gutierrez-Nava, M. P. Carreón, J.-F. Eckert, M. Luccisano, C. Schall, P. Masson, J.-L. Gallani, B. Heinrich, D. Guillon, and J.-F. Nierengarten, *Helv. Chim. Acta*, **85**, 288 (2002). d) T. Konishi, M. Fujitsuka, H. Luo, Y. Araki, O. Ito, and L. Y. Chiang, *Fullerenes, Nanotubes, and Carbon Nanostructures*, **11**, 237 (2003).

17 L. Echegoyen and M. A. Herranz, "Fullerenes: From Synthesis to Optoelectronic Properties," ed by D. M. Guldi and N. Martín, Kluwer Academic Publishers (2002), Chap. 9.

18 C. Luo, M. Fujitsuka, A. Watanabe, O. Ito, L. Gan, Y. Huang, and C. H. Huang, *J. Chem. Soc., Faraday Trans.*, **94**, 527 (1998).

19 a) M. M. Alam, A. Watanabe, and O. Ito, *J. Photochem. Photobiol., A*, **104**, 59 (1997). b) M. M. Alam, A. Watanabe, and O. Ito, *Bull. Chem. Soc. Jpn.*, **70**, 1833 (1997). c) M. M. Alam, O. Ito, N. Sakurai, and H. Moriyama, *Fullerene Sci. Technol.*, **6**, 1007 (1998). d) M. M. Alam, O. Ito, N. Sakurai, and H. Moriyama, *Res. Chem. Intermed.*, **25**, 323 (1999).

20 N. Armaroli, G. Accorsi, J.-P. Gisselbercht, M. Cross, V. Krasnikov, D. Tsamouras, G. Hadziioannou, M. J. Gómez-Escalonilla, F. Langa, J.-F. Eckert, and J.-F. Neirengarten, *J. Mater. Chem.*, **12**, 2077 (2002).

21 a) L. Huchet, S. Akoudad, E. Levillain, J. Roncali, A. Emge, and P. Bäuerle, *J. Phys. Chem. B*, **102**, 7776 (1998). b) R. Andreu, J. Garin, and J. Orduna, *Tetrahedron*, **57**, 7883 (2001). c) E. Allard, J. Cousseau, J. Oruduna, J. Garin, H. Luo, Y. Araki, and O. Ito, *Phys. Chem. Chem. Phys.*, **4**, 5944 (2002).

22 a) A. Watanabe and O. Ito, *J. Phys. Chem.*, **98**, 7736 (1994). b) O. Ito, Y. Sasaki, Y. Yoshikawa, and A. Watanabe, *J. Phys. Chem.*, **99**, 9838 (1995).